

A LINEAR LEAST-SQUARES MFS FOR CERTAIN ELLIPTIC PROBLEMS

YIORGOS-SOKRATIS SMYRLIS AND ANDREAS KARAGEORGHIS

ABSTRACT. The Method of Fundamental Solutions (MFS) is a boundary-type meshless method for the solution of certain elliptic boundary value problems. In this work, we propose an efficient algorithm for the linear least-squares version of the MFS, when applied to the Dirichlet problem for certain second order elliptic equations in a disk. Various aspects of the method are discussed and a comparison with the standard MFS is carried out. Numerical results are presented.

1. INTRODUCTION

In the MFS, the solution is approximated by a linear combination of fundamental solutions of the operator of the partial differential equation of the problem under consideration. This approximation thus satisfies the differential equation and the coefficients in the linear combination are determined from the boundary conditions. The satisfaction of the boundary conditions can be done in two ways: One way is by fixing and preassigning the locations of the singularities and simply collocating the boundary conditions. This leads to a linear system with the same number of equations as unknowns or a linear least-squares problem. Alternatively, the locations of the singularities can be determined along with the coefficients, which results in a non-linear least-squares problem. Details and applications of these formulations can be found in the recent survey papers [2, 3, 5]. A description of the linear least-squares MFS can be found in Golberg and Chen [4], Kolodziej [6, 7] and Ramachandran [9]. In this paper, we consider the formulation resulting in the linear least-squares problem.

The paper is organized as follows. In Section 2, we present the MFS formulation for general second order linear elliptic boundary value problems, subject to Dirichlet boundary conditions and the corresponding least-squares problem which results in a square linear system. In Section 3, we present an efficient algorithm for the solution of this system in the case of Laplace's equation in a disk. The efficiency of this algorithm relies on the special structure of resulting matrix. In Section 4, we present numerical examples.

2000 *Mathematics Subject Classification.* Primary 65N12, 65N38; Secondary 65N15, 65T50, 65Y99.

Key words and phrases. Method of fundamental solutions, linear least-squares method, boundary meshless methods, elliptic boundary value problems.

Finally, in Section 5 we give some concluding remarks and discuss possible applications and extensions of the method.

2. THE LINEAR LEAST-SQUARES MFS

We consider the boundary value problem

$$\begin{cases} Lu = 0 & \text{in } \Omega, \\ u = f & \text{on } \partial\Omega, \end{cases} \quad (2.1)$$

where L is a second order linear elliptic operator, Ω is an open bounded domain in \mathbb{R}^2 . In the MFS, the solution is approximated by

$$u_N(\mathbf{c}, \mathbf{Q}; P) = \sum_{j=1}^N c_j k(P, Q_j), \quad P \in \bar{\Omega}, \quad (2.2)$$

where $\mathbf{c} = (c_1, c_2, \dots, c_N)^T$ and \mathbf{Q} is a $2N$ -vector containing the coordinates of the singularities Q_j , $j = 1, \dots, N$, which lie on the boundary $\partial\Omega'$, of the domain Ω' , where $\bar{\Omega} \subset \Omega'$. The function $k(P, Q)$ is a fundamental solution of the elliptic operator L . The satisfaction of the boundary condition is imposed on a set of boundary points $\{P_i\}_{i=1}^M$:

$$u_N(\mathbf{c}, \mathbf{Q}; P_i) = f(P_i), \quad i = 1, \dots, M. \quad (2.3)$$

This yields the linear system

$$G\mathbf{c} = \mathbf{f},$$

where the elements of the $M \times N$ matrix G are given by

$$g_{i,j} = k(P_i, Q_j), \quad i = 1, \dots, M, \quad j = 1, \dots, N.$$

If $M > N$, we seek a least-squares solution of this system, i.e. the N coefficients c_1, \dots, c_N , which minimize the quadratic functional

$$\Phi(c_1, \dots, c_N) = \sum_{i=1}^M \left| \sum_{j=1}^N c_j k(P_i, Q_j) - f(P_i) \right|^2.$$

Therefore, these coefficients c_1, \dots, c_N must satisfy the *normal equations*

$$\frac{\partial}{\partial c_j} \Phi(c_1, \dots, c_N) = 0, \quad j = 1, \dots, N,$$

or equivalently

$$\sum_{i=1}^M k(P_i, Q_j) \left\{ \sum_{j=1}^N c_j k(P_i, Q_j) - f(P_i) \right\} = 0, \quad j = 1, \dots, N,$$

that is

$$G^*G\mathbf{c} = G^*\mathbf{f}, \quad (2.4)$$

where G^* is the transpose of G .

3. EFFICIENT IMPLEMENTATION

We consider the special case of Laplace's equation in the disk of radius ϱ , i.e. $L \equiv \Delta$ and

$$\Omega = B_\varrho = \{\mathbf{x} \in \mathbb{R}^2 : |\mathbf{x}| < \varrho\},$$

with boundary $\partial\Omega = S_\varrho = \{\mathbf{x} \in \mathbb{R}^2 : |\mathbf{x}| = \varrho\}$. The fundamental solution k is given by

$$k(P, Q) = -\frac{1}{2\pi} \log |P - Q|, \quad (3.1)$$

with $|P - Q|$ denoting the distance between the points P and Q . The singularities Q_j^α are fixed on the boundary S_R of the disk B_R concentric to B_ϱ , where $R > \varrho$. A set of collocation points $\{P_i\}_{i=1}^M$, where $M \geq N$, is placed on S_ϱ . If $P_i = (x_{P_i}, y_{P_i})$, then we take

$$x_{P_i} = \varrho \cos \frac{2(i-1)\pi}{M}, \quad y_{P_i} = \varrho \sin \frac{2(i-1)\pi}{M}, \quad i = 1, \dots, M.$$

The locations of the singularities, $Q_j^\alpha = (x_{Q_j^\alpha}, y_{Q_j^\alpha})$ are defined by

$$x_{Q_j^\alpha} = R \cos \left(\frac{2(j-1)\pi}{N} + \frac{2\alpha\pi}{M} \right), \quad y_{Q_j^\alpha} = R \sin \left(\frac{2(j-1)\pi}{N} + \frac{2\alpha\pi}{M} \right), \quad (3.2)$$

where $j = 1, \dots, N$. The positions of the singularities differ by an angle $\frac{2\pi\alpha}{M}$ from the positions of the boundary points and $0 \leq \alpha < 1$. In the case $\alpha \neq 0$, we thus have a *rotation* of the singularities with respect to the boundary points (see [10]) and hence the introduction of the superscript α for the Q_j 's. The elements of the matrix G_α are given by

$$g_{i,j}^\alpha = -\frac{1}{2\pi} \log |P_i - Q_j^\alpha|, \quad i = 1, \dots, M, \quad j = 1, \dots, N. \quad (3.3)$$

In the case when M is an integer multiple of N , i.e. $M = mN$ with $m \in \mathbb{N}$, the matrix G_α has the form (dropping the α 's)

$$G_\alpha = \begin{pmatrix} g_{1,1} & g_{1,2} & \cdots & g_{1,N} \\ g_{2,1} & g_{2,2} & \cdots & g_{2,N} \\ \vdots & \vdots & & \vdots \\ g_{m,1} & g_{m,2} & \cdots & g_{m,N} \\ \hline g_{1,N} & g_{1,1} & \cdots & g_{1,N-1} \\ g_{2,N} & g_{2,1} & \cdots & g_{2,N-1} \\ \vdots & \vdots & & \vdots \\ g_{m,N} & g_{m,1} & \cdots & g_{m,N-1} \\ \hline g_{1,N-1} & g_{1,N} & \cdots & g_{1,N-2} \\ \vdots & \vdots & & \vdots \\ g_{m,N-1} & g_{m,N} & \cdots & g_{m,N-2} \\ \hline \cdots \\ \hline g_{1,2} & g_{1,3} & \cdots & g_{1,1} \\ \vdots & \vdots & & \vdots \\ g_{m,2} & g_{m,3} & \cdots & g_{m,1} \end{pmatrix} \begin{array}{l} \text{row 1} \\ \text{row 2} \\ \vdots \\ \text{row } m \\ \hline \text{row } m+1 \\ \text{row } m+2 \\ \vdots \\ \text{row } 2m \\ \hline \text{row } 2m+1 \\ \vdots \\ \text{row } 3m \\ \hline \cdots \\ \hline \text{row } (N-1)m+1 \\ \vdots \\ \text{row } Nm \end{array}$$

We observe that row $m+1$ is a rotation of row 1, row $2m+1$ is a rotation of row $m+1$ and in general row $\mu m + \kappa$ is a $\mu - \nu$ rotation of row $\nu m + \kappa$ for $\kappa = 1, \dots, m$. In other words, the matrices consisting of rows $\kappa, m + \kappa, 2m + \kappa, \dots, (N-1)m + \kappa$ for $\kappa = 1, \dots, m$ are circulant matrices [1].

3.1. Diagonalization of the matrix $G_\alpha^* G_\alpha$. We next investigate the efficient diagonalization of the matrix $G_\alpha^* G_\alpha$. In order to achieve this, we must first examine the matrix $U_M G_\alpha U_N^*$, where

$$U_N^* = \frac{1}{\sqrt{N}} \begin{pmatrix} 1 & 1 & 1 & \cdots & 1 \\ 1 & \omega & \omega^2 & \cdots & \omega^{N-1} \\ 1 & \omega^2 & \omega^4 & \cdots & \omega^{2N-1} \\ \vdots & \vdots & \vdots & & \vdots \\ 1 & \omega^{N-1} & \omega^{2(N-1)} & \cdots & \omega^{(N-1)(N-1)} \end{pmatrix},$$

with $\omega_N = e^{\frac{2\pi i}{N}}$. The matrix U_N is clearly unitary and its conjugate transpose is known as the *Fourier matrix*.

If we set $h_j = g_{j,1}$, $j = 1, \dots, M$, and let λ_j , $j = 1, \dots, M$, be the eigenvalues of the matrix $H = \text{circ}(h_1, \dots, h_M)$ then we have the expression (see [1])

$$\lambda_j = \sum_{k=1}^M h_k \omega_M^{(j-1)(k-1)}. \quad (3.4)$$

The matrix $U_M G_\alpha$ is then

$$\frac{1}{\sqrt{M}} \begin{pmatrix} \bar{\lambda}_1 & \bar{\lambda}_1 & \bar{\lambda}_1 & \cdots & \bar{\lambda}_1 \\ \bar{\lambda}_2 & \bar{\omega}_M^m \bar{\lambda}_2 & \bar{\omega}_M^{2m} \bar{\lambda}_2 & \cdots & \bar{\omega}_M^{(N-1)m} \bar{\lambda}_2 \\ \vdots & \vdots & \vdots & \vdots & \vdots \\ \bar{\lambda}_N & \bar{\omega}_M^{(N-1)m} \bar{\lambda}_N & \bar{\omega}_M^{2(N-1)m} \bar{\lambda}_N & \cdots & \bar{\omega}_M^{(N-1)(N-1)m} \bar{\lambda}_N \\ \bar{\lambda}_{N+1} & \bar{\lambda}_{N+1} & \bar{\lambda}_{N+1} & \cdots & \bar{\lambda}_{N+1} \\ \vdots & \vdots & \vdots & \vdots & \vdots \\ \bar{\lambda}_{2N} & \bar{\omega}_M^{(2N-1)m} \bar{\lambda}_{2N} & \bar{\omega}_M^{2(2N-1)m} \bar{\lambda}_{2N} & \cdots & \bar{\omega}_M^{(N-1)(2N-1)m} \bar{\lambda}_{2N} \\ \vdots & \vdots & \vdots & \vdots & \vdots \\ \bar{\lambda}_{(m-1)N+1} & \bar{\lambda}_{(m-1)N+1} & \bar{\lambda}_{(m-1)N+1} & \cdots & \bar{\lambda}_{(m-1)N+1} \\ \vdots & \vdots & \vdots & \vdots & \vdots \\ \bar{\lambda}_{mN} & \bar{\omega}_M^{(mN-1)m} \bar{\lambda}_{mN} & \bar{\omega}_M^{2(mN-1)m} \bar{\lambda}_{mN} & \cdots & \bar{\omega}_M^{(N-1)(mN-1)m} \bar{\lambda}_{mN} \end{pmatrix};$$

that is,

$$(U_M G_\alpha)_{k,\ell} = \frac{1}{\sqrt{M}} \bar{\omega}_M^{m(k-1)(\ell-1)} \bar{\lambda}_k,$$

where $k = 1, \dots, M$ and $\ell = 1, \dots, N$. Post-multiplication of $U_M G_\alpha$ by U_N^* yields the $M \times N$ matrix

$$U_M G_\alpha U_N^* = \frac{1}{\sqrt{m}} \begin{pmatrix} \bar{\lambda}_1 & 0 & 0 & 0 & \cdots & 0 & 0 \\ 0 & \bar{\lambda}_2 & 0 & 0 & \cdots & 0 & 0 \\ 0 & 0 & \bar{\lambda}_3 & 0 & \cdots & 0 & 0 \\ \vdots & \vdots & \vdots & \vdots & & \vdots & \vdots \\ 0 & 0 & 0 & 0 & \cdots & \bar{\lambda}_{N-1} & 0 \\ 0 & 0 & 0 & 0 & \cdots & 0 & \bar{\lambda}_N \\ \bar{\lambda}_{N+1} & 0 & 0 & 0 & \cdots & 0 & 0 \\ 0 & \bar{\lambda}_{N+2} & 0 & 0 & \cdots & 0 & 0 \\ \vdots & \vdots & \vdots & \vdots & & \vdots & \vdots \\ 0 & 0 & 0 & 0 & \cdots & 0 & \bar{\lambda}_{2N} \\ \vdots & \vdots & \vdots & \vdots & & \vdots & \vdots \\ 0 & 0 & 0 & 0 & \cdots & 0 & \bar{\lambda}_{mN} \end{pmatrix};$$

that is,

$$(U_M G_\alpha U_N^*)_{k,\ell} = \frac{1}{\sqrt{m}} \delta_{k,\ell}^N \bar{\lambda}_k,$$

where

$$\delta_{k,\ell}^N = \begin{cases} 1 & \text{if } k \equiv \ell \pmod{N} \\ 0 & \text{if } k \not\equiv \ell \pmod{N}. \end{cases}$$

Finally,

$$\begin{aligned} (U_M G_\alpha U_N^*)^* U_M G_\alpha U_N^* &= U_N G_\alpha^* U_M^* U_M G_\alpha U_N^* = U_N G_\alpha^* G_\alpha U_N^* \\ &= \text{diag}(\mu_1, \dots, \mu_N) := \Lambda, \end{aligned}$$

where

$$\mu_\ell = \frac{1}{m} \sum_{j=1}^m |\lambda_{(j-1)N+\ell}|^2. \quad (3.5)$$

The μ_ℓ , $\ell = 1, \dots, N$, are the eigenvalues of G^*G . We have thus obtained the diagonalization of $G_\alpha^*G_\alpha$:

$$G_\alpha^*G_\alpha = U_N^* \Lambda U_N. \quad (3.6)$$

The following theorem guarantees the solvability of (2.4).

Theorem 3.1. *For every $N \in \mathbb{N}$, $\alpha \in [-\frac{1}{2}, \frac{1}{2}]$ and $m \geq 2$, the matrix $G_\alpha^*G_\alpha$ is nonsingular.*

PROOF. This follows from Theorem 2.11 of [11] according to which the only possibly vanishing eigenvalues among the λ_j , $j = 1, \dots, M$, are

- (i) $\lambda_1(\alpha)$, which may occur only for $\alpha \in (-\frac{1}{6}, \frac{1}{6})$, and
 (ii) $\lambda_{M/2+1}(\frac{1}{2})$, if M is even.

Clearly, for $m = M/N \geq 2$, formula (3.5) shows that no eigenvalue μ_ℓ , $\ell = 1, \dots, N$, vanishes. \square

System (2.4) may be written as

$$U_N G_\alpha^* G_\alpha U_N^* U_N \mathbf{c} = U_N G_\alpha^* U_M^* U_M \mathbf{f},$$

or equivalently,

$$\Lambda \hat{\mathbf{c}} = \hat{G}_\alpha^* \hat{\mathbf{f}}, \quad (3.7)$$

where $\hat{\mathbf{c}} = U_N \mathbf{c}$, $\hat{G}_\alpha^* = U_N G_\alpha^* U_M^*$ and $\hat{\mathbf{f}} = U_M \mathbf{f}$. Thus, if $\hat{\mathbf{f}} = (\hat{f}_1, \dots, \hat{f}_M)$ and $\hat{\mathbf{c}} = (\hat{c}_1, \dots, \hat{c}_N)$, the ℓ -th element of the vector $\hat{G}_\alpha^* \hat{\mathbf{f}}$ is given by

$$\left(\hat{G}_\alpha^* \hat{\mathbf{f}} \right)_\ell = \frac{1}{\sqrt{m}} \sum_{j=1}^m \lambda_{(j-1)N+\ell} \hat{f}_{(j-1)N+\ell}, \quad (3.8)$$

where $\ell = 1, \dots, N$. Therefore, the solution of (3.7) is given by

$$\hat{c}_\ell = \sqrt{m} \frac{\sum_{j=1}^m \lambda_{(j-1)N+\ell} \hat{f}_{(j-1)N+\ell}}{\sum_{j=1}^m |\lambda_{(j-1)N+\ell}|^2}, \quad \ell = 1, \dots, N. \quad (3.9)$$

If we now let

$$k_j(P) = k(P, Q_j^\alpha), \quad j = 1, \dots, N,$$

and $\mathbf{k} = (k_1(P), \dots, k_N(P))$, then (2.2) becomes

$$u_N(P) = \sum_{j=1}^N c_j k_j(P) = \langle \mathbf{c}, \mathbf{k} \rangle = \langle U_N \mathbf{c}, U_N \mathbf{k} \rangle = \langle \hat{\mathbf{c}}, \hat{\mathbf{k}} \rangle,$$

where $\langle \cdot, \cdot \rangle$ is the inner product in \mathbb{C}^N .

Remark 3.1. In the case $m = 1$, i.e., $M = N$, formula (3.9) reduces to

$$\hat{c}_\ell = \frac{\hat{f}_\ell}{\bar{\lambda}_\ell}, \quad \ell = 1, \dots, N.$$

Further, (2.2) takes the form

$$u_N(P) = \sum_{\ell=1}^N \frac{1}{\bar{\lambda}_\ell} \hat{f}_\ell \bar{\hat{c}}_\ell.$$

3.2. The algorithm. The following algorithm which calculates the approximate solution (2.2):

Step 1: Compute $\hat{\mathbf{f}} = U_M \mathbf{f}$.

Step 2: Compute the eigenvalues $\lambda_j, j = 1, \dots, M$, from (3.4).

Step 3: Compute the vector $\hat{\mathbf{c}}$ from (3.9).

Step 4: Compute $\hat{\mathbf{k}} = U_N \mathbf{k}$.

We observe the following:

Remarks 3.2.

- (i) In **Step 1**, because of the form of the matrix U_M , the operation is equivalent to performing a Discrete Fourier Transform (DFT) of dimension M . This can be done at a cost of $O(M \log M)$ operations via an appropriate Fast Fourier Transform (FFT) algorithm. In **Step 2**, we first calculate the eigenvalues $\lambda_j, j = 1, \dots, M$, of the matrix $\text{circ}(h_1, \dots, h_M)$, at a cost of $O(M \log M)$ operations. Subsequently, we need an additional $O(M)$ operations to calculate the vector $\hat{\mathbf{c}}$. In **Step 3**, the vector $\hat{\mathbf{c}}$ can be computed at a cost of $O(M)$ operations. Finally in **Step 4**, because of the form of the matrix U_N^* , the operation can be carried out via inverse FFTs at a cost of $O(N \log N)$ operations. The total cost is therefore $O(M \log M)$.
- (ii) In the proposed algorithm, the circulant nature of the matrix $G_\alpha^* G_\alpha$ enables us to solve the corresponding system with $O(M \log M)$ operations instead of $O(N^3)$ for standard Gauss elimination. It should be noted that it is essential for the ratio M/N to be an integer, otherwise the resulting matrix $G_\alpha^* G_\alpha$ is not, in general, circulant. For example, if $M = 3, N = 2$, then

$$G_\alpha^* G_\alpha = \begin{pmatrix} g_{11} & g_{12} \\ g_{21} & g_{22} \end{pmatrix}$$

where

$$\begin{aligned} g_{11} &= |\lambda_1(0)|^2 + |\lambda_2(0)|^2 + |\lambda_3(0)|^2, \\ g_{22} &= |\lambda_1(\frac{1}{2})|^2 + |\lambda_2(\frac{1}{2})|^2 + |\lambda_3(\frac{1}{2})|^2, \end{aligned}$$

and the $\lambda_j(\alpha)$ are given by (3.4) for $M = 3$. One can easily verify that in general $g_{11} \neq g_{22}$.

- (iii) Ramachandran [9] uses a Singular Value Decomposition (SVD) method for the solution of (2.4). This approach is applicable to arbitrary domains and has a cost of $O(MN^2)$ operations.

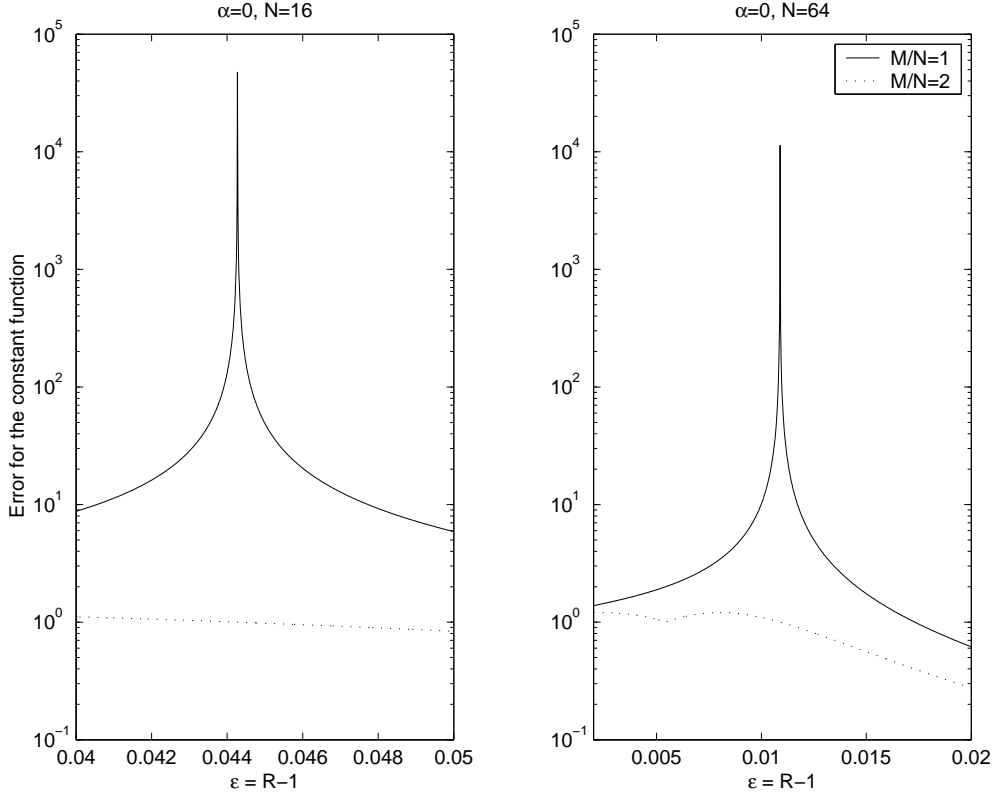


FIGURE 1. Elimination of the singular point at $R = 2^{1/N}$ for the constant function.

- (iv) *The efficient algorithm we propose is only applicable when the domain we are considering is a disk, but can be applied to different second-order elliptic operators with radial symmetry. For example, in the case of the Helmholtz equation*

$$\Delta u + \lambda^2 u = 0,$$

the fundamental solution is

$$k(P, Q) = -\frac{i}{4} H_0^{(2)}(\lambda |P - Q|),$$

where $H_0^{(2)}$ is the Hankel function of order 2. Clearly, the corresponding matrix $G_\alpha^ G_\alpha$ is also circulant. For further details and other examples of such fundamental solutions, see [8].*

4. NUMERICAL RESULTS

We consider problems with complex boundary data which correspond to analytic functions $u^R + iu^I$ on the unit disk. The real and imaginary parts of these functions are treated separately. We examine two types of problems:

- Problems with boundary data corresponding to exact solutions of the form $u = z^k = r^k e^{ik\vartheta}$, $k \in \mathbb{N}$. These problems are important as they represent the Fourier frequencies of the boundary data on a circle. The study of the error for such problems reveals the behaviour the method for more general problems.
- Problems with boundary data corresponding to exact solutions of the form

$$u(z) = \frac{1}{z - \beta},$$

where $\beta > 1$. The boundary data have a full Fourier spectrum and these problems are important because the behaviour of the solution changes dramatically as β approaches 1.

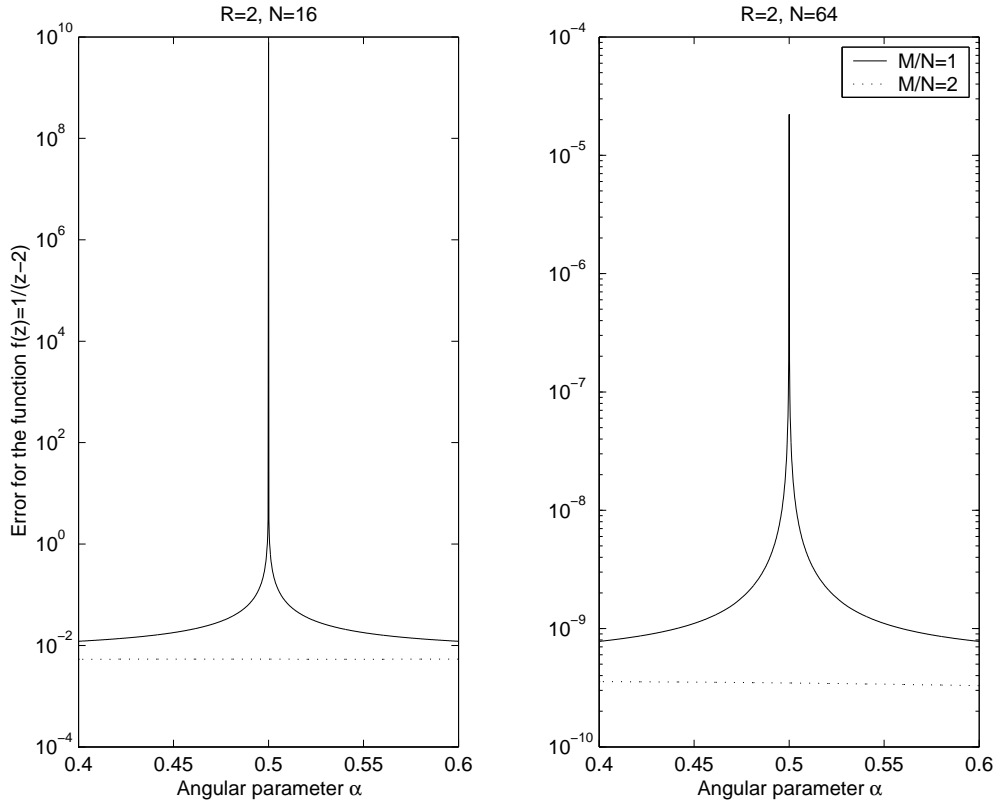


FIGURE 2. Elimination of the singular point at $\alpha = 1/2$ for N even.

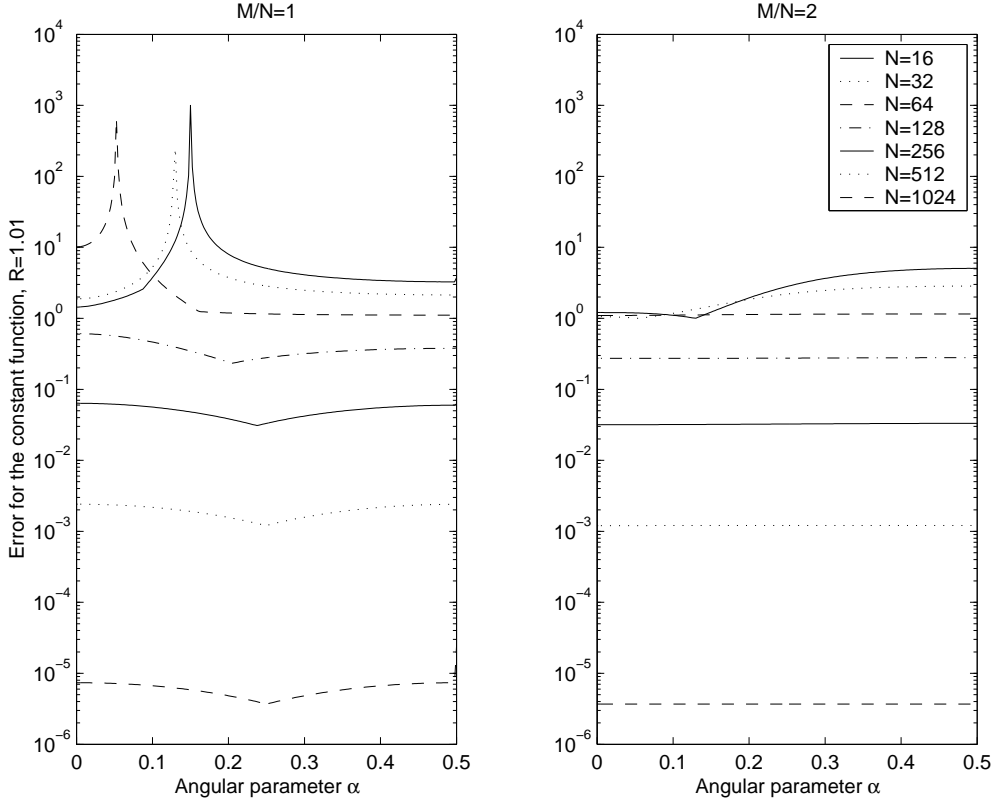


FIGURE 3. Dependence of the error on the angular parameter for $M/N = 1, 2$.

For each problem, we calculated the maximum relative error

$$E = \frac{\|u^R - u_N^R\|_\infty + \|u^I - u_N^I\|_\infty}{\|u\|_\infty},$$

where u_N^R , u_N^I are the MFS approximations to u^R and u^I , respectively. The maximum relative error was calculated on a uniform grid of 1001 points on the boundary (since all the functions involved are harmonic and the maximum principle holds) defined by

$$(\cos \theta_j, \sin \theta_j), \quad \theta_j = \frac{2\pi(j-1)}{1001}, \quad j = 1, \dots, 1001.$$

In Figure 1, we present the error versus $\varepsilon = R - 1$ for the constant function (i.e. $f \equiv 1$) when the angular parameter $\alpha = 0$ in the cases $N = 16, 64$ for $M/N = 1, 2$ respectively. From this figure, one may observe that the vanishing of the first eigenvalue, which occurs when $R = 2^{1/N}$, and which is visible as a peak in the case $M/N = 1$, is eliminated when $M/N = 2$. The elimination of this singularity persists for larger integer values of M/N .

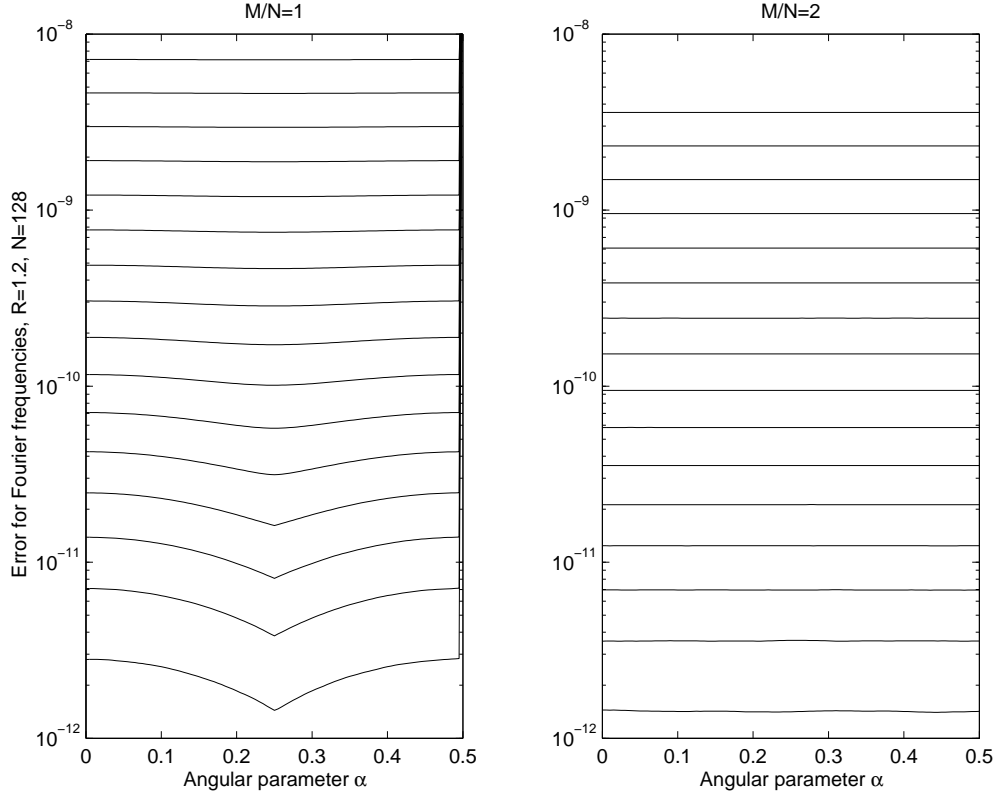


FIGURE 4. Dependence of the error for the first 16 Fourier frequencies ($f = e^{ik\vartheta}$, $k = 1, \dots, 16$), on angular parameter α for $M/N = 1, 2$.

This phenomenon was also observed for different integer values of M/N . This is a direct consequence of Theorem 3.1.

Similarly, in Figure 2, we present the error versus the angular parameter α for the function $f(z) = \frac{1}{z-2}$, when $R = 2$, $N = 16, 64$ and $M/N = 1, 2$ respectively. Again one may observe that the vanishing of the first eigenvalue occurring when N is even at $\alpha = 1/2$ and appears as a peak in the case $M/N = 1$, is eliminated when $M/N = 2$. The same phenomenon was also observed for different values of N . This is again a direct consequence of Theorem 3.1.

In Figure 3, we compare the error for the constant function versus α for $R = 1.01$ for various values of N in the cases $M/N = 1, 2$. Apart from the fact that the peaks indicating singularities are avoided when $M/N = 2$, we also observe a slight improvement in the accuracy in this case. Also, the dependence of the error on α is much less significant in the case $M/N = 2$. Identical observations were made for larger integer values of M/N .

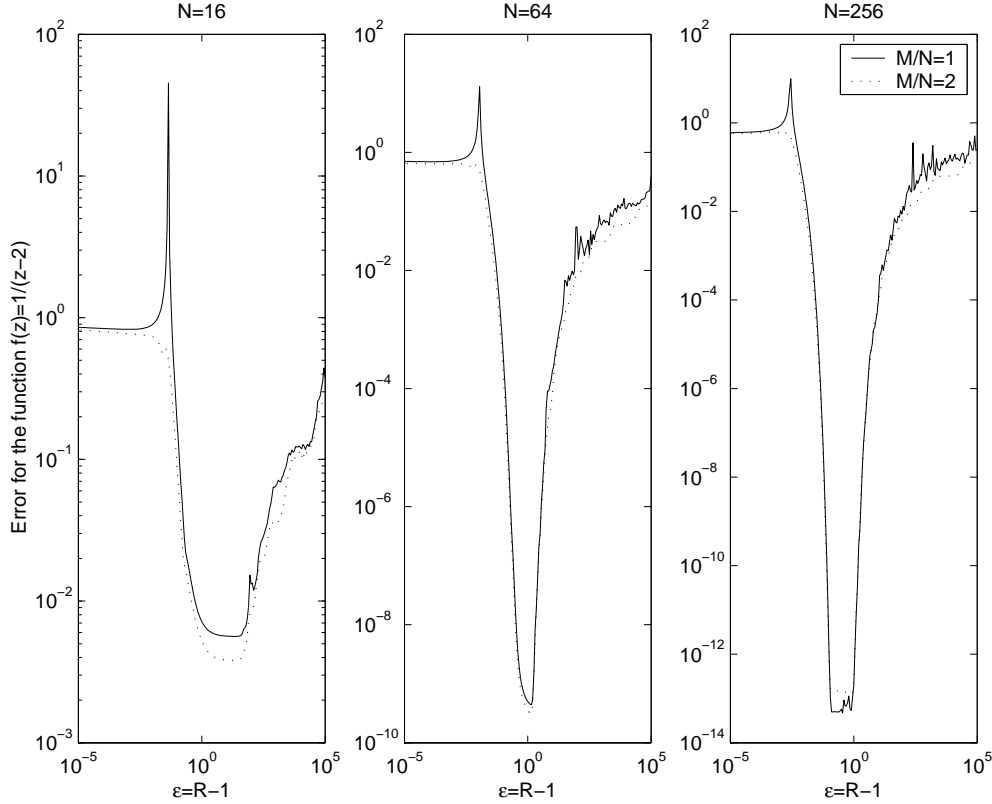


FIGURE 5. Dependence of the error on $\varepsilon = R - 1$ for the function $f(z) = \frac{1}{z-2}$ for $\alpha = 0$, $N = 16, 64, 256$ and $M/N = 1, 2$.

In Figure 4, we show the dependence on α of the error for the first 16 Fourier frequencies (i.e., $f = e^{ik\vartheta}$, $k = 1, \dots, 16$), for $R = 1.2$, $N = 128$, when $M/N = 1, 2$, respectively. In this figure, the frequencies appear from the bottom to the top as k increases. We observe that the dependence on the error of the angular parameter is much weaker in the case $M/N = 1$. Also, the singularities at $\alpha = 1/2$ which are visible for $M/N = 1$, are avoided when $M/N = 2$. Further, we observe a slight improvement in the accuracy which becomes more significant for high frequencies. The corresponding graphs for larger integer values of M/N are identical.

In Figure 5, we present the error versus $\varepsilon = R - 1$ for the function $f(z) = 1/(z - 2)$, for $\alpha = 0$, $N = 16, 64, 256$ and $M/N = 1, 2$. Apart from the slight improvement in the accuracy, we also observe that in the case $M/N = 2$, we avoid the singularity peak. Similar results are observed in Figure 6, where we deal with the much less *regular* function $f(z) = 1/(z - 1.01)$. In this case, the improvement, when $M/N = 2$, is much more visible than in the previous example, because in the less regular function, there is a more

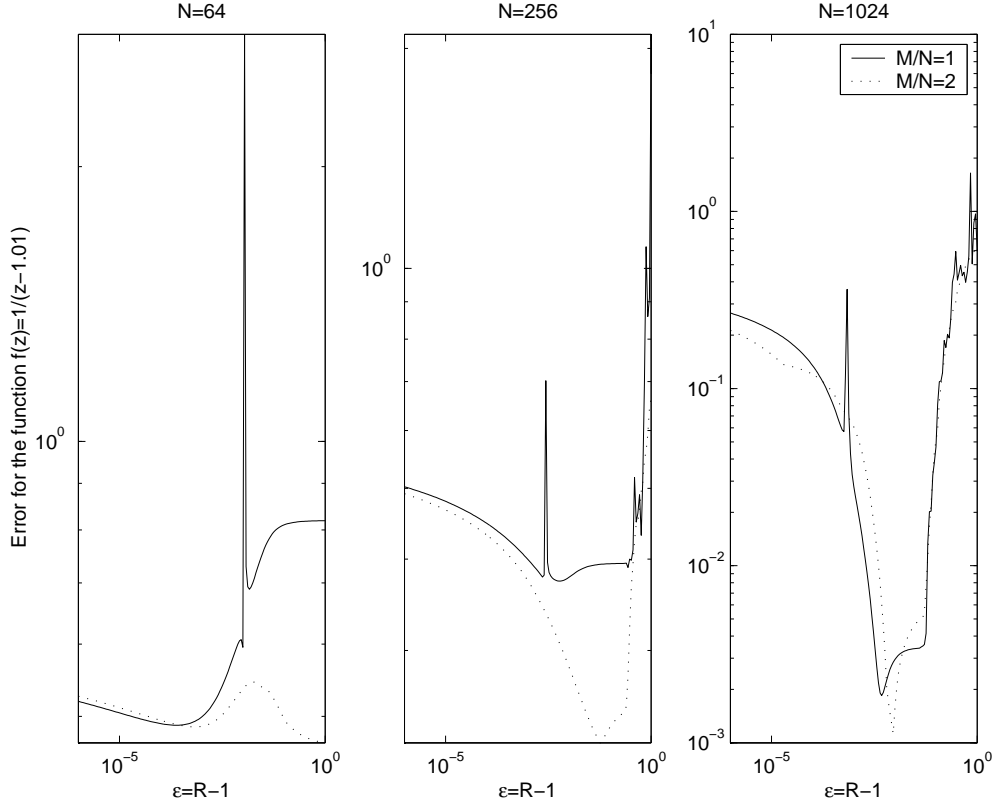


FIGURE 6. Dependence of the error on $\epsilon = R - 1$ for the function $f(z) = \frac{1}{z-1.01}$ for $\alpha = 0$, $N = 16, 64, 256$ and $M/N = 1, 2$.

significant contribution of high Fourier frequencies. Once again, identical results were observed for larger integer values of M/N .

In Figure 7, we present the error versus $\epsilon = R - 1$ for the first sixteen Fourier frequencies (i.e. $f = e^{ik\theta}$, $k = 1, \dots, 16$), for $\alpha = 0$, $N = 128$, when $M/N = 2$. In this figure, the frequencies appear from the bottom to the top as k increases. The interval of values of ϵ for which high accuracy is attained is reduced as $|k|$ increases.

Finally, in Figure 8, we present the error versus $\epsilon = R - 1$ for various Fourier frequencies, for $\alpha = 0$, $N = 32$, when $M/N = 1, 2$. Here we observe that the improvement of the accuracy when $M/N = 2$, becomes more significant as the frequency increases.

The gradual deterioration in the approximation as R increases, observed in Figures 5, 6 and, especially, 7 and 8, is caused by roundoff errors in the calculation of the eigenvalues λ_j , $j = 1, \dots, M$, via DFT. In particular, in the simplest case when $\alpha = 0$, Theorem 2.6

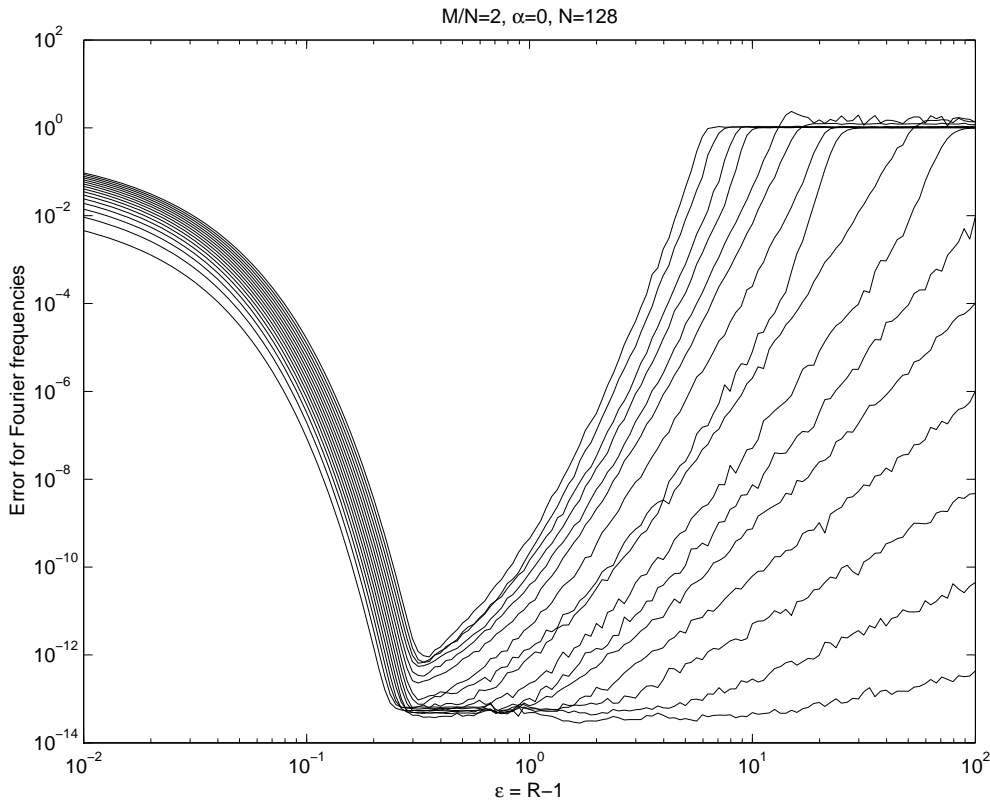


FIGURE 7. Dependence of the error on $\varepsilon = R - 1$ for the first 16 Fourier frequencies ($f = e^{ik\vartheta}$, $k = 1, \dots, 16$).

in [11], implies, that for $j = 2, \dots, M/2$, we have the following asymptotic form:

$$\lambda_j(0) = \frac{M}{4\pi} \cdot \frac{1}{(j-1)R^{j-1}} + O(R^{-N+j-1}).$$

Clearly, FFT cannot reproduce these values when they are smaller than the machine accuracy.

5. SUMMARY

In this paper, we propose an efficient linear least-squares MFS algorithm for the solution of elliptic problems on a disk subject to Dirichlet boundary conditions. The linear least-squares MFS is applicable for any $M \geq N$. However, an efficient algorithm can only be developed when the number of boundary points M is an integer multiple of the number of singularities N . The algorithm relies on the properties of circulant matrices and, in particular, their efficient inversion via FFT. When $M/N \geq 2$, the proposed algorithm has certain advantages over the standard MFS (i.e., when $M = N$). In particular, unlike the

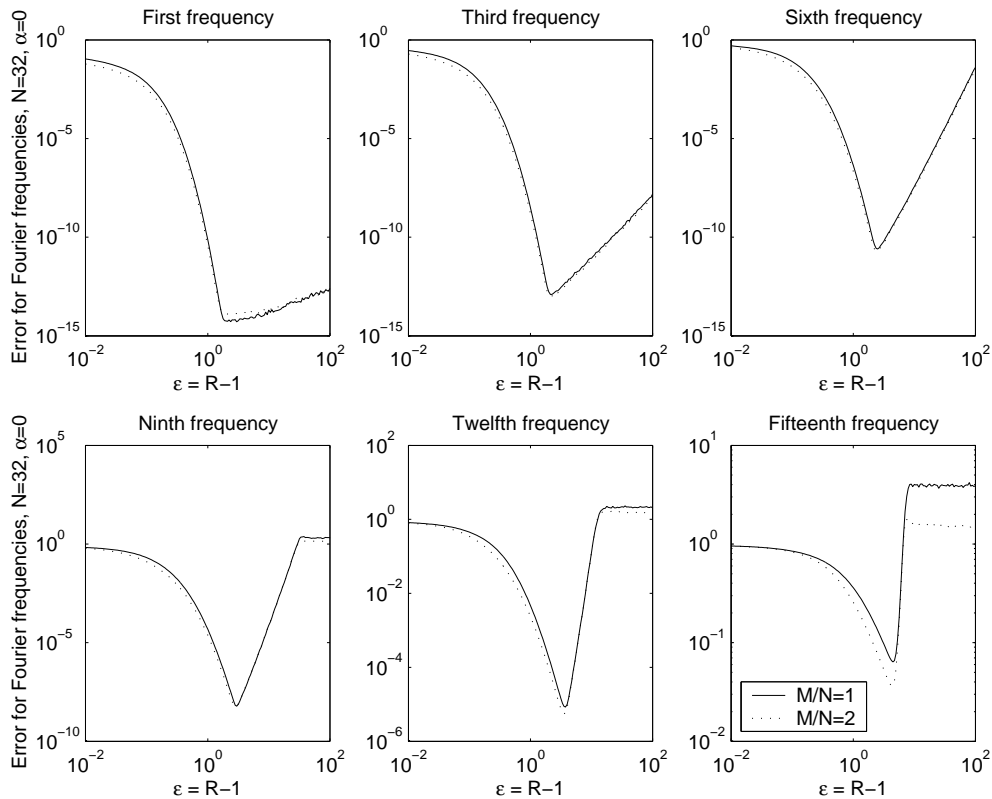


FIGURE 8. Dependence of the error on $\varepsilon = R - 1$ for various Fourier frequencies.

standard MFS in which the resulting matrix might be singular, the linear system resulting when $M/N \geq 2$ is always solvable. Also, there is an improvement in the accuracy of the method when either the angular parameter α or the distance R are varied. This improvement is more significant for higher Fourier frequencies. As a result, we obtain better approximations for more realistic boundary data which may exhibit lower regularity. Experiments were carried out for $M/N = 1$ and $M/N = 2$. Interestingly, the results obtained for $M/N = 2$ and $M/N = m > 2$, were virtually identical. This method is also applicable to other second order elliptic operators, such as the Helmholtz equation.

REFERENCES

- [1] P.J. DAVIS, *Circulant Matrices*, John Wiley & Sons, New York, 1979.
- [2] G. FAIRWEATHER AND A. KARAGEORGHIS, *The method of fundamental solutions for elliptic boundary value problems*, Adv. Comput. Math., **9**, 69–95, 1998.
- [3] G. FAIRWEATHER, A. KARAGEORGHIS AND P. A. MARTIN, *The method of fundamental solutions for scattering and radiation problems*, Engng. Analysis with Boundary Elements, to appear.

- [4] M. A. GOLBERG AND C. S. CHEN, *Discrete Projection Methods for Integral Equations*, Computational Mechanics Publications, Southampton, 1996.
- [5] M. A. GOLBERG AND C. S. CHEN, *The method of fundamental solutions for potential, Helmholtz and diffusion problems*, in: *Boundary Integral Methods and Mathematical Aspects*, ed. M. A. Golberg, WIT Press/Computational Mechanics Publications, Boston, 103–176, 1999.
- [6] J. A. KOLODZIEJ, *Review of applications of the boundary collocation methods in mechanics of continuous media*, *Solid Mech. Arch.*, **12**, 187–231, 1987.
- [7] J. A. KOLODZIEJ, *Applications of the Boundary Collocation Method in Applied Mechanics*, Wydawnictwo Politechniki Poznanskiej, Poznan, 2001. (In Polish).
- [8] P.K. KYTHE, *Fundamental Solutions for Differential Operators and Applications*, Birkhäuser, Boston, 1996.
- [9] P. A. RAMACHANDRAN, *Method of fundamental solutions: singular value decomposition analysis*, *Commun. Numer. Meth. Engng.*, **18**, 789–801, 2002.
- [10] Y.S. SMYRLIS AND A. KARAGEORGHIS, *Some aspects of the method of fundamental solutions for certain harmonic problems*, *J. Sci. Comput.*, **16**, 341–371, 2001.
- [11] Y.S. SMYRLIS AND A. KARAGEORGHIS, *Numerical analysis of the MFS for certain harmonic problems*, Technical report TR/04/2003, Department of Math. & Stat., University of Cyprus. (See <http://www.ucy.ac.cy/~smyrlis/Papers/IMAJNA.ps>).

DEPARTMENT OF MATHEMATICS AND STATISTICS, UNIVERSITY OF CYPRUS/ΠΑΝΕΠΙΣΤΗΜΙΟ ΚΥΠΡΟΥ,
P.O.Box 20537, 1678 NICOSIA/ ΛΕΥΚΩΣΙΑ, CYPRUS/ ΚΥΠΡΟΣ
E-mail address: smyrlis@ucy.ac.cy, andreask@ucy.ac.cy